

A hybrid method of simulating broadband ground motion: A case study of the 2006 Pingtung earthquake, Taiwan



Y. T. Yen, C. T. Cheng, K. S. Shao & P. S. Lin
Sinotech Engineering Consultants Inc., Taipei, Taiwan, ROC.

K. F. Ma
Institute of Geophysics, National Central University, Zhongli, Taiwan, ROC.

Y. C. Wu & C. W. Chang
Institute of Nuclear Energy Research, Taiwan, ROC.

SUMMARY:

We applied the hybrid method to validate the strong ground motion of the 2006 Pingtung earthquake in Taiwan. Considering relative small events which contain path and site effect in waveforms as Green's functions can resolve the problem of lack of precise velocity structure to replace the path effect. Characterized slip model provided source parameters needed for the ground motion prediction. Alternatively, a stochastic Green's function (SGF) method can be employed when the empirical Green's Functions were unavailable. Further, the long period can be obtained numerically by the Frequency-Wavenumber (FK) method. Broadband frequency strong ground motion could be calculated by combining the FK method for the low-frequency simulation and the SGF method for high-frequency simulation. A nuclear power plant in southern of Taiwan was experienced strong shaking by this earthquake. The adjacent stations and assumed sites were to be as the case for possibility evaluation of predicting ground motion utilizing the hybrid method.

Keywords: strong ground motion, empirical green's function, stochastic green's function, hybrid method, the 2006 Pingtung earthquake

1. INSTRUCTIONS

The purpose of achieving accurate strong ground motion prediction is for hazard evaluation in specific sites, especially, the nationally critical infrastructures. Strong ground motion producing by earthquake sources could be appropriately modeled, as the heterogeneous slip distribution and rupture propagating properties over the fault plane were well known. The MaanShan Nuclear Power Plant (MaanShan NPP) in Taiwan was attacked by an earthquake occurred on December 26, 2008 with moment magnitude 6.9. The risk of seismic hazard still exists even though no damage happened in this event. Preventing or mitigating possible earthquake-induced damage for NPP induced by future earthquakes must be carefully evaluated because the Manila subducting system is very close to the MaanShan NPP. Kamae et al. (1998) have proposed a method of simulating the broadband waveforms in which the source parameters, such as the size of asperities, seismic moment, and stress drop and so on were quantified by forward modeling using the empirical Green's function method. The individual high- and low-frequency simulation skill was considered. Their simulation scheme applied into the 1995 Hyogoken-Nambu Earthquake and succeeded to recover broadband strong ground motions including the short-period bands for the observations recording from the earthquake (Kamae and Irikura, 1998). In this study, we implemented the empirical Green's function method to obtain an optimum characterized slip model for broadband strong ground motion evaluation of the 2006 Pingtung Earthquake offshore southwest Taiwan. Future, we verified the observations near NPP field through comparing the fitness between observed and synthetic waveforms derived by the characterized slip model using the empirical Green's function method. Finally, broadband strong ground motion waveforms at assumed sites within NPP were obtained using hybrid scheme.

2. DATA

2.1. Observations near the NPP

Taiwan Strong Motion Instrumentation Program (TSMIP) governed by Central Weather Bureau (CWB) had recorded plentiful of observation data for 2006 Pingtung earthquake. Four stations recorded by seismic network were considered for validation of synthetic waveforms simulated by hybrid method. They are located on the place where their epicenter distance is between 50 and 100 km. Fig. 2.1 and 2.2 show the spatial distribution of seismic station, nuclear power plant and hypocenter. The value peak ground acceleration (PGA) of two horizontal components in four observed stations is in the range from around 100 to 324 gal. The value PGV is around 20 cm/sec. Obviously, the value PGA for the stations on the west side of Nuclear Power Plant is larger than the ones for the stations on the east side. We could recognize one pulse in the displacement waveforms, suggesting that one asperity is expected for this earthquake.

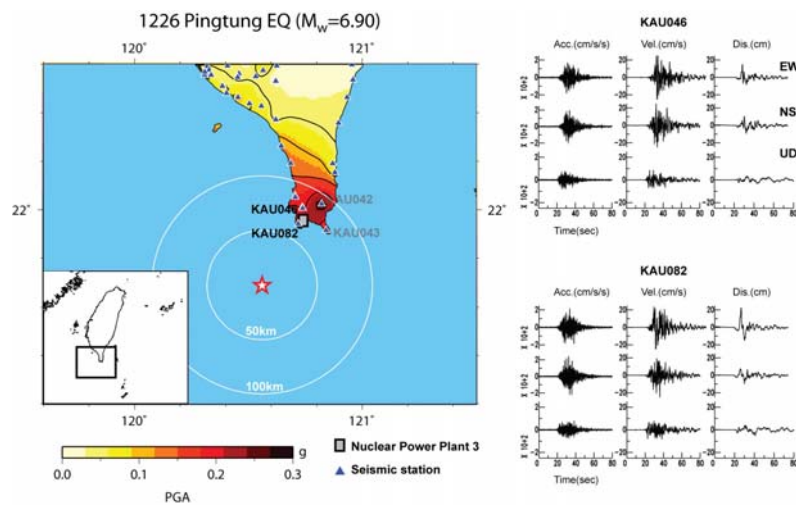


Figure 2.1. Spatial distribution and acceleration, velocity and displacement waveforms of KAU046 and KAU082 stations. Red star shows the hypocenter.

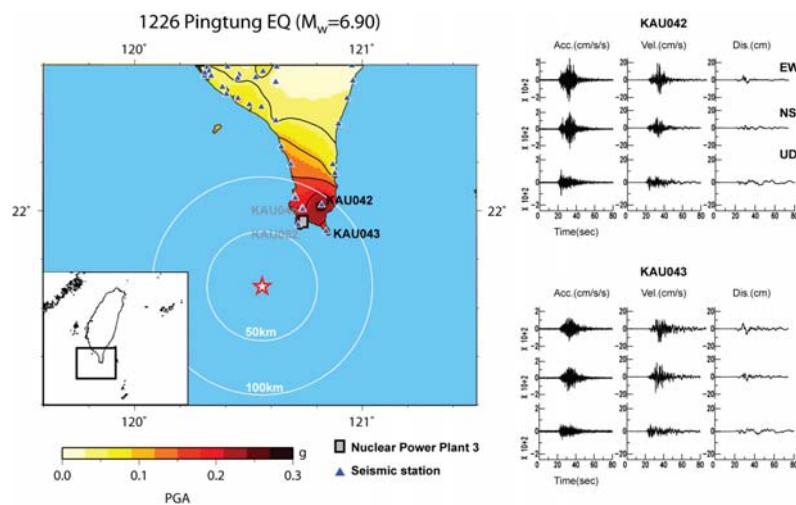


Figure 2.2. Spatial distribution and acceleration, velocity and displacement waveforms of KAU042 and KAU043 stations. Red star shows the hypocenter.

3. SIMULATION METHOD

Following the scheme proposed by Kamae et al. 1998, the scheme of hybrid method to simulate broadband ground motion is shown as Fig. 3.1.

3.1. Low frequency (<1Hz)

We simulated the low-frequency waveforms of an assumed point source within a layer velocity structure according to the algorithm of Frequency-Wavenumber (FK) method (Zhu and Rivera, 2002), in which the Green's functions of a point source or a subevent are calculated based on elastic wave-propagation theory in horizontally layered medium. Considering the reliability of velocity structure, we adopted the result of Wu et al. in 2009 which had considered the aftershocks of 2006 Pingtung earthquake to enhance the resolution of our study region.

3.2. High frequency (>1Hz)

For high frequency waveform simulation, we implement the stochastic method (Motazedian and Atkinson, 2005). The attenuation effects of the propagation path are considered by an empirical Q of quality factor and geometric-spreading attenuation models. We assumed the frequency-dependent $Q=117f^{0.77}$, estimated from coda waves, and geometric spreading in the form $1/R^b$, where $b = 1.0$ for $R < 50$ km, $b= 0$ for $50 \text{ km} \leq R < 150$ km, and $b=0.5$ for $R \geq 150$ km, which was previously used in Taiwan region for the Chi-Chi earthquake (Roumelioti and Beresnev, 2003). For the site correction of study area, we adopted an amplification function for genic-rock sites (Boore and Joyner, 1997). According the results of Beresnev (2002), the amplification function for soil-sites could be considered as two times of average ratio between soil- and rock- sites.

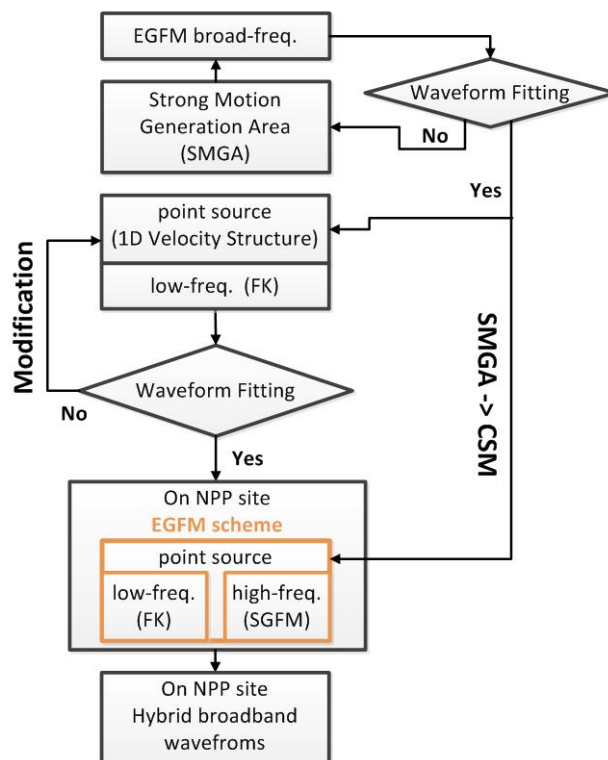


Figure 3.1. The scheme of hybrid simulation of broadband prediction waveforms.

4. RESULT

4.1. Characterized slip model

We estimate the characterized slip model using the empirical Green's function method (EGFM) (Irikura, 1983; 1986). Broadband, two horizontal components of acceleration, velocity and displacement waveforms were simulated by EGFM to compare with recorded waveforms at four observed stations (KAU046, KAU082, KAU042, KAU043). Site condition classified by Lee and Tsai (2008) and location of seismic stations show in Table 4.1. Small event (em6) that location and focal mechanism are similar to target event, 2006 Pingtung earthquake, is chosen to be as empirical Green's function. Source parameters of target event and small event are shown in Table 4.2. The upper and lower limit of the frequency range used in this simulation was 0.5 and 8 Hz, respectively. The lower limit was determined by the appropriate signal-to-noise ratio of the small event data. Characterized slip model with one asperity area of 20 x 20 km² (i.e. strong motion generation area (SMGA)) was determined by inspecting a certain range of parameters (e.g., rupture velocity, rise time and the location of starting point) once the best fitting with minimum residuals of displacement waveforms and those of envelopes of acceleration waveforms. Comparing the slip model with the one of Yen et al. (2008) and Lee et al. (2008), it shows coincident region of the asperity near hypocenter (Fig. 4.1).

Table 4.1. Site condition and location of observed and assumed stations

Station Code	Site Class*	Latitude(°)	Longitude(°)
KAU082	D2	21.942	120.719
KAU046	D2	22.006	120.738
KAU042	C3	22.024	120.821
KAU043	C3	21.914	120.840
NPP001	D2	21.956	120.740
NPP002	D2	21.956	120.730
NPP003	D2	21.966	120.740
NPP004	D2	21.956	120.745

* The classification from Lee and Tsai (2008)

Table 4.2. Parameters for characterizing slip model

	Earthquake parameters	
	1226 Event	em6
Date	2006/12/26 12:26(UT)	2009/10/11 06:42(UT)
Location	120.560E 21.69N	120.629E 21.928N
Depth (km)	41.11	42.00
Magnitude (Mw)	6.9	4.4
Seismic moment (dyne-cm)	2.7×10^{26}	5.05×10^{22}
Focal mechanism (degree) (strike, dip, rake)	335, 75, -98	336, 56, -99
Parameters for empirical Green's function method		
The length of SMGA (km)	20	
The width of SMGA (km)	20	
The ratio of stress drop	2.39	
Rupture velocity (km/sec)	2.7	
Rise time (sec)	0.9	

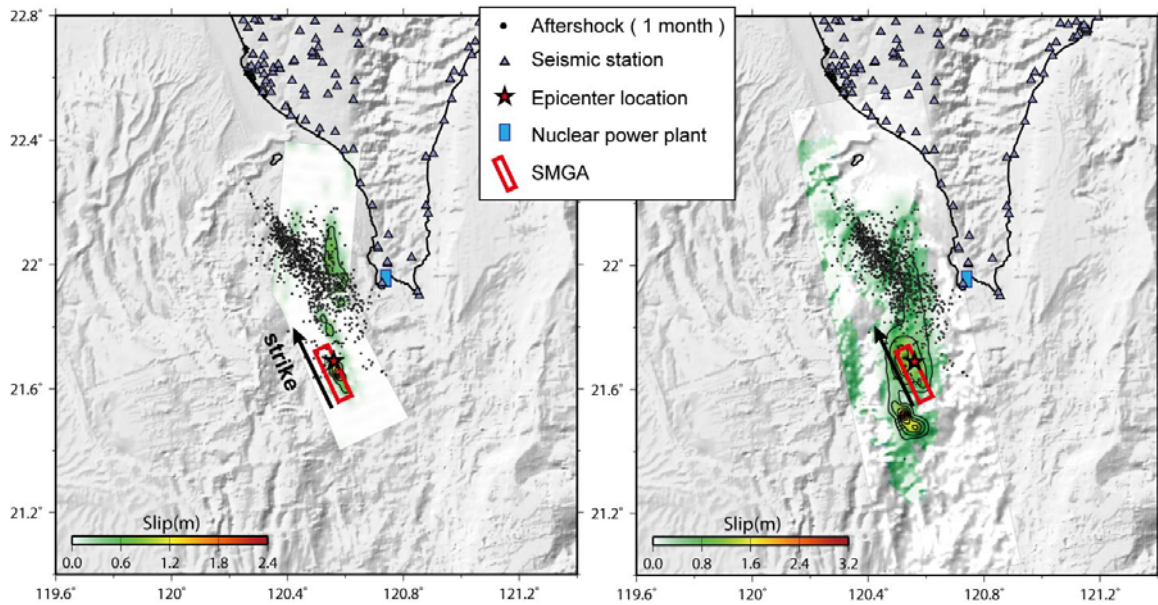


Figure 4.1. Comparison between the strong motion generation area of this study and the slip model inverted by teleseismic data (Left: Yen et al., 2008) and strong motion (Right: Lee et al. 2008).

4.2. Prediction of broadband ground motion

Based on the result of characterizing slip model, the strong motion generation area was estimated as shown in Fig. 4.2.1. Here, the hybrid Green's function (HGF) is to combine the low-frequency portion from FK method and the high-frequency portion from stochastic method. The source parameters of the em6 event were taken for simulating the hybrid broadband ground motion of hypothetical point source, including location, depth and focal mechanism. We implemented the empirical Green's function method to calculate the broadband synthetic waveforms, in which the waveforms of real small event to be as empirical Green's function are replaced by the HGF. The broadband synthetic waveforms and Fourier acceleration spectra at the location of four observed seismic stations were obtained and shown as Fig. 4.2.2. The waveforms of two horizontal components of acceleration, velocity and displacement in time domain roughly well fit with observed ones. Two stations at west-side NPP represented that a difference of amplitude between synthetic and observed acceleration spectra in lower frequency is obvious for soil sites. However, two rock site stations at east-side NPP show that the fitting is relatively well. It can be found that there are obvious mismatch in the amplitude around 1 Hz from comparison between synthetic and observed Fourier acceleration spectra for stations of KAU046 and KAU082.

For understanding possible ground motion, we placed assumed seismic station at four specific locations within MaanShan NPP field. Fig. 4.2.3 shows estimated time history of broadband ground motions at each assumed sites near NPP field. Those points are adjacent to NPP with short distance of about 2 km. The range of estimated peak accelerations of the horizontal and vertical component at NPP001 to NPP004 is between 239 and 504 Gal and between 147 and 171 Gal, respectively.

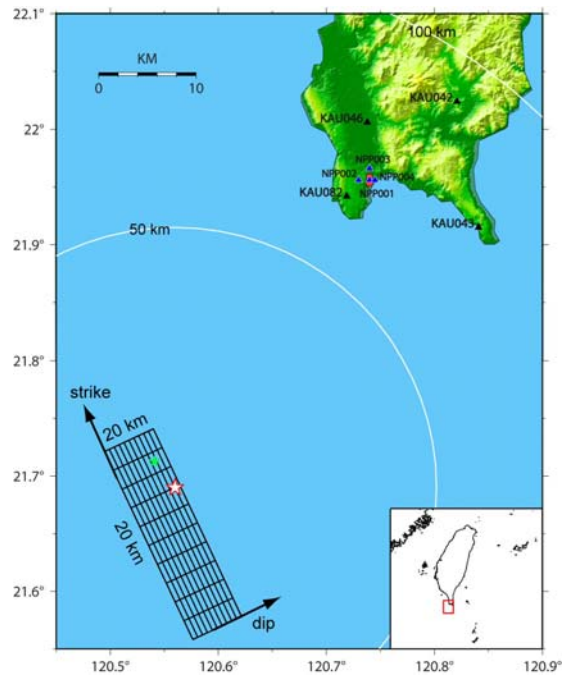


Figure 4.2.1. Map showing the spatial distribution of the SMGA of 2006 Pingtung earthquake (rectangular grid) and seismic observed stations, KAU046, KAU082, KAU042 and KAU043 (black triangular), assumed stations near NPP, NPP001~4 (blue triangles). Red and green stars shows the hypocenter and starting point of SMGA, respectively.

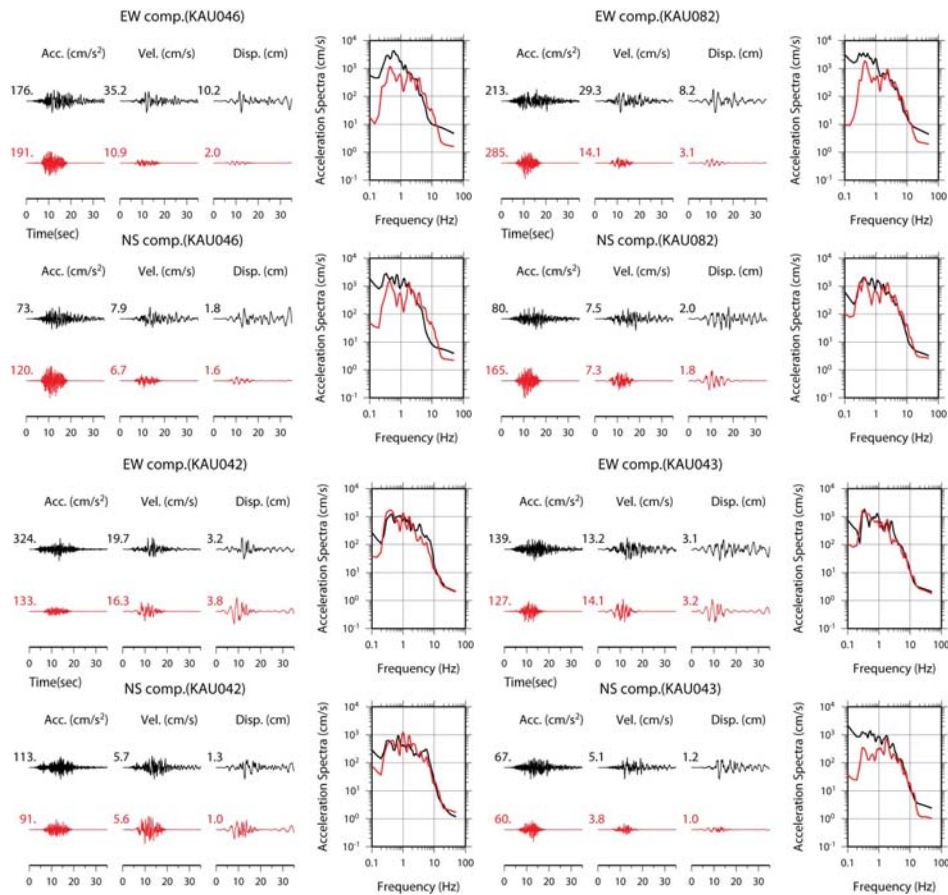


Figure 4.2.2. Synthetic waveforms and Fourier acceleration spectra with hybrid method for four observed stations.

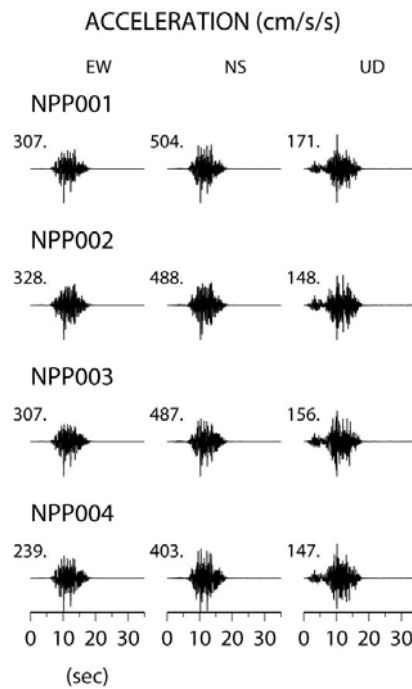


Figure 4.2.3. Synthetic waveforms for four stations within MaanShan NPP site.

5. DISCUSSION AND CONCLUSIONS

We validated broadband waveforms based on the simulation of hybrid Green's function method for 2006 Pingtung earthquake, in that the characterized slip model with one asperity was used to calculate the synthetic waveforms. We found a well agreement between the observed and predicted waveforms was obtained at C3 sites that geological condition belongs to very dense soil and soft rock. However, the agreement was considerably decreased at D2 sites which belong to stiff soils due to the lack of considering shallow soil layer for low-frequency portion of predicted waveforms. In acceleration This suggests that shallow layer of velocity structure have to carefully concern for low frequency simulation. Otherwise, the SMGA just was considered for a frequency band of 0.5 to 8 Hz so that possible contribution of low-frequency from off-SMGA region might be ignored to lead to the error of simulation.

A series of hybrid strong ground motion simulations at MaanShan NPP sites have been carried out to estimate the PGAs at four representative locations within NPP field via applying characterized source model with simple one asperity for 2006 Pingtung earthquake. The capability of the simulation model and the appropriateness of the key parameters used in the simulations have been confirmed by simulating the ground motions recorded at observed stations around the NPP during the 2006 Pingtung earthquake in the southwest offshore Taiwan. The results are essential for future probabilistic and deterministic seismic hazard analyses.

ACKNOWLEDGEMENT

The strong motion waveform data of TSMIP and relocated aftershocks are provided by Central Weather Bureau of Taiwan. We thank Prof. Zhu and Prof. Motazedian provided the simulation programs. This research was supported by the Institute of Nuclear Energy Research of Taiwan.

REFERENCES

- Beresnev, I.A. (2002). Nonlinearity at California generic soil sites from modeling recent strong-motion data, *Bull. Seism. Soc. Am.* **92**, 863-870.
- Boore, D.M., and Joyner W.B. (1997). Site amplifications for generic rock sites, *Bull. Seismol. Soc. Am.* **87**, 327-341.
- Irikura, K. (1983). Semi-empirical estimation of strong ground motions during large earthquakes, *Bull. Disast. Prev. Res. Inst., Kyoto Univ.* **33**, 63-104.
- Irikura, K. (1986). Prediction of strong acceleration motions using empirical Green's function, *Proc. 7th Japan Earthq. Eng. Symp.*, 151-156, 1986.
- Kamae, K., Irikura K. and Pitarka, A. (1998). A technique for simulating strong ground motion using hybrid Green's function, *Bull. Seismol. Soc. Am.* **88**, 2, 357-367.
- Kamae, K. and Irikura K. (1998). Source model of the 1995 Hyogo-ken Nanbu earthquake and simulation of near-source ground motion, *Bull. Seismol. Soc. Am.* **88**, 2, 400-412.
- Lee, C.T. and Tsai, B.R. (2008). Mapping Vs30 in Taiwan. *Terr. Atmos. Ocean. Sci.* **19**, 671-682.
- Lee, S.J., Liang, W.T. and Huang, B.S. (2008). Source mechanisms and rupture processes of the 26 December 2006 Pingtung earthquake doublet as determined from the regional seismic records. *Terr. Atmos. Ocean. Sci.* **19**, 555-565, doi: 10.3319/TAO.2008.19.6.555(PT).
- Motazedian, D., Atkinson, G.M. (2005). Stochastic finite-fault modelling based on a dynamic corner frequency. *Bull. Seismol. Soc. Am.* **95**, 995-1010.
- Roumelioti, Z. and Beresnev, I.A. (2003). Stochastic finite-fault modeling of ground motions from the 1999 Chi-chi, Taiwan, earthquake: Application to rock and soil sites with implications for nonlinear site response, *Bull. Seism. Soc. Am.* **93**, 1691-1702.
- Yen, Y.T., Ma K.F. and Wen Y.Y. (2008). Slip partition of the 26 December 2006 Pingtung, Taiwan (M 6.9, M6.8) earthquake doublet determined from teleseismic waveforms. *Terr. Atmos. Ocean. Sci.* **19**, 567-578, doi:10.3319/TAO.2008.19.6.567(PT).
- Zhu, L. and Rivera, L.A. (2002). A note on the dynamic and static displacements from a point source in multi-layered media. *Geophys. J. Int.* **148**, 619-627.